UDC 621.314 https://doi.org/10.20998/2074-272X.2024.5.04

L. Djafer, R. Taleb, F. Mehedi

# Dspace implementation of real-time selective harmonics elimination technique using modified carrier on three phase inverter

***Introduction.*** *In the contemporary world, alternative electrical energy has become an integral part of our daily existence, with the majority of our electrical materials, electronic devices, and industrial equipment relying on this energy source. Consequently, ensuring the quality of the electrical signal obtained is of paramount importance in the process of converting and distributing electrical energy. The improvement of the output voltage inverter can be achieved through adjustments to the inverter structure or by refining the control strategy.* ***The novelty*** *of the presented research lies in an innovative approach that employs real-time modulation for efficient control over the reduction of harmonics, alongside managing the fundamental component. This approach is applicable to both bipolar and unipolar configurations, featuring quarter-wave and half-wave symmetries.* ***Purpose.*** *Employing this modulation strategy aims to enhance the durability of the switching components and enhance the voltage output of the inverter.* ***Methods.*** *The methodology is founded on a sine-sine modulation as its foundational model. It constitutes an inventive pulse width modulation technique in which a reference sinusoidal waveform, operating at the desired signal frequency, is compared to a modified carrier signal with an identical time period as the reference signal.* ***Results.*** *This paper introduces a broader and more comprehensive approach, alongside specific solutions, for the control and mitigation of harmonics in three phase voltage source inverters. The proposed method offers precise control over the reduction of harmonics and the fundamental component, and it can be implemented in extensive power electronic converters.* ***Practical value.*** *To assess the effectiveness of the given control approach, we conducted simulations as well as real-time implementation employing Dspace DS1104 controller board. The outcomes were highly favorable, confirming the effectiveness and validity of the suggested control algorithm.* References 15, tables 4, figures 7.
*Key words:* **voltage source inverter, real-time harmonics control, pulse width modulation technique, Dspace DS1104.**

***Вступ***. *У сучасному світі альтернативна електрична енергія стала невід'ємною частиною нашого повсякденного існування, і більшість наших електричних матеріалів, електронних пристроїв і промислового обладнання покладаються на це джерело енергії. Отже, забезпечення якості отриманого електричного сигналу має першочергове значення в процесі перетворення та розподілу електричної енергії. Покращення вихідної напруги інвертора може бути досягнуто шляхом коригування структури інвертора або вдосконалення стратегії керування.* ***Новизна*** *представленого дослідження полягає в інноваційному підході, який використовує модуляцію в реальному часі для ефективного контролю над зменшенням гармонік, поряд з керуванням основною компонентою. Цей підхід застосовний як до біполярних, так і до однополярних конфігурацій, що мають чвертьхвильову та напівхвильову симетрію.* ***Мета***. *Застосування цієї стратегії модуляції спрямоване на підвищення довговічності комутаційних компонентів і підвищення вихідної напруги інвертора.* ***Методи***. *Методологія базується на синусоїдній модуляції як базовій моделі. Він являє собою метод широтно-імпульсної модуляції за винаходом, у якій опорна синусоїдальна форма хвилі, що працює на бажаній частоті сигналу, порівнюється з модифікованим несучим сигналом з ідентичним періодом часу, що й опорний сигнал.* ***Результати***. *Ця стаття представляє ширший і комплексний підхід, поряд із конкретними рішеннями, для контролю та пом'якшення гармонік у трифазних інверторах джерел напруги. Запропонований метод пропонує точний контроль над зменшенням гармонік і основної складової, і він може бути реалізований у потужних електронних перетворювачах.* ***Практична цінність***. *Щоб оцінити ефективність даного підходу до управління, ми провели моделювання, а також реалізацію в реальному часі з використанням плати контролера Dspace DS1104. Результати були дуже сприятливими, підтверджуючи ефективність і валідність запропонованого алгоритму контролю.* Бібл. 15, табл. 4, рис. 7.
*Ключові слова:* **інвертор джерела напруги, контроль гармонік у реальному часі, метод широтно-імпульсної модуляції, Dspace DS1104.**

**Abbreviations**

| | | | |
|---|---|---|---|
| FFT | Fast Fourier Transform | RTHC | Real-Time Harmonics Control |
| GA | Genetic Algorithm | RTI | Real-Time Implementation |
| PWM | Pulse Width Modulation | SHE-PWM | Selective Harmonic Elimination Pulse Width Modulation |
| RTHE | Real-Time Harmonic Elimination | SPWM | Sinusoidal Pulse Width Modulation |

**Introduction.** Harmonics and the frequency at which switches operate present notable difficulties within power systems overall, with switching converters being particularly affected [1]. To tackle this issue, two commonly used approaches are the widely recognized SPWM and SHE-PWM [2–5].

SHE-PWM, regarded as a substitute for the SPWM approach, has been extensively studied and explored over time. When compared to SPWM and SHE-PWM provides enhanced control over the lower order harmonic and results in a reduced switching frequency, consequently prolonging the converter's operational lifespan [6]. Another significant distinction between the two methodologies lies in the manner in which the angles of switching are computed. Within the SPWM technique, angles are continuously produced in real-time through the comparison of a sinusoidal reference with the triangular carrier. In SHE-PWM, the computations are carried out offline, rendering its implementation less resource-intensive. The primary difficulty linked with SHE-PWM lies in the resolution of the resulting system of nonlinear equations [6]. To simplify these equations, prior and contemporary studies have relied on essential assumptions that enforce quarter-wave symmetry on the output waveform [2, 3].

SHE-PWM involves a two-step procedure. In the first phase, the switching instants are determined by solving a system of nonlinear algebraic transcendental equations [7], which can be accomplished using various algorithms like the commonly used iterative method, elimination theory, and a range of optimization

approaches, involving GAs and particle swarm optimization techniques. During the second phase, the computed switching instants are stored in a lookup table for real-time retrieval [7]. In practice look-up tables are electronic memories, there capacities depend on the number of harmonics desired to be eliminated and the sampling time of the modulation index. In recent times, numerous studies have put forward various SHE-PWM methods that eliminate the need for storing switching angles in memory, as discussed in references [7, 8]. The approaches introduced in references [9, 10] are regarded as significant advancements in the concept of RTHE.

**The goal of the paper** is analysis, simulation and implementation RTHC method on three phase inverter, this method permits the removal of chosen harmonics while also simplifying the generation and comparison of the modified sine carrier and a sinusoidal reference.

**Subject of investigations.** This paper presents an innovative method for managing and reducing harmonics within switching converters, known as RTHE. It is introduced as an alternate approach to SHE-PWM [11, 12]. This approach employs a modulation strategy that utilizes an altered sine carrier waveform, which is contrasted with a typical sine wave, rather than the more common triangular carrier wave [12]. As a result, RTHC streamlines the process of generating and comparing modified sine carrier and the reference sinusoid modulation signals, allowing for quick and precise execution without any precision-related concerns.

In pursuit of this objective, the switching instants are calculated by solving nonlinear algebraic transcendental equations with the use of any optimization algorithm (this paper employs GA). Then these computed angles are applied to produce the required sine carrier wave, resulting in a sine-sine modulation.

**Sine-sine PWM.** Figure 1,*a* shows the electrical circuit of a three phase inverter, where the input voltage is denoted as $v_{dc}$ and 6 electronic switches. To generate a PWM signal, two sinusoidal waveforms are employed: a reference sinusoid denoted as $v_{ref} = m_i \cdot \sin(2 \cdot \pi \cdot f \cdot t + \pi)$ and a sinusoidal carrier labeled as $v_{car} = m_i \cdot \sin k \cdot (2 \cdot \pi \cdot f \cdot t)$ as shown in Fig. 1,*b* juxtaposed with (rather than a sinusoidal reference and a triangular carrier as in traditional SPWM). The PWM waveform that emerges from this contrast is shown in Fig. 1,*c* with a maximum amplitude of $r = 1$, a fixed value of $k = 9$ and a frequency $f = 50$ Hz. The constant $k$ signifies the relationship between the carrier frequency and the reference signal frequency. A generalized method to compute the intersection points, as presented in Fig. 1,*b*,*c*, in the context of sine-sine PWM, involves solving (1). The angles of intersection $\varphi_i$ are represented in radians for the values of $k = 5, 9, 13, 17, 21, 25, \ldots, n, n+4$:

$$\varphi_i = \frac{i \cdot \pi}{(k + (-1)^i)}, \quad i = \left[1 : \frac{k-1}{2}\right], \qquad 0 < \varphi_i > \frac{\pi}{2}, \quad k = 5, 9, 13, 17, 21 \ldots n, n+4. \tag{1}$$

Table 1 illustrates instances of intersection points in a sine-sine PWM signal for various $k$ values ranging from 5 to 21.

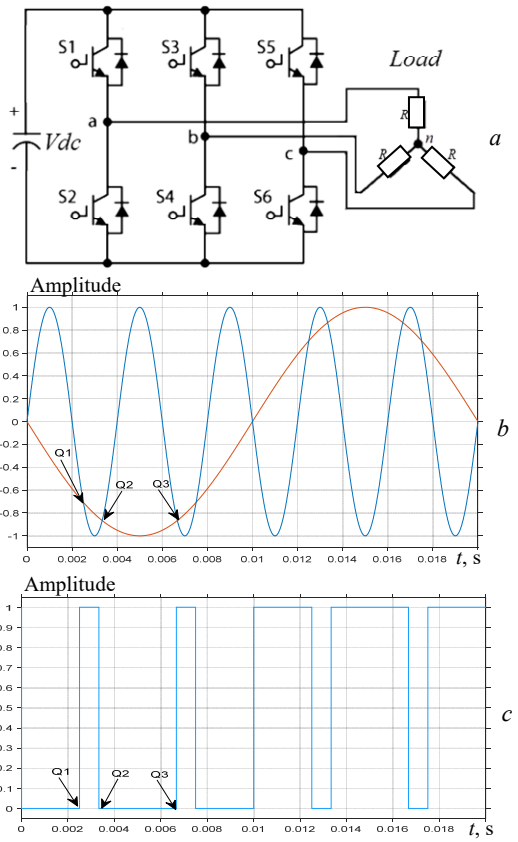


Fig. 1. Sine-sine PWM: *a* – electrical circuit of three phase inverter; *b* – sine-wave comparison; *c* – produced PWM

Table 1

Points of intersection present in a sine-sine PWM signal

| | $k = 5$ | $k = 9$ | $k = 13$ | $k = 17$ | $k = 21$ |
|---|---|---|---|---|---|
| $\varphi_1$ | $\pi/4$ | $\pi/8$ | $\pi/12$ | $\pi/16$ | $\pi/20$ |
| $\varphi_2$ | $\pi/3$ | $\pi/5$ | $\pi/7$ | $\pi/9$ | $\pi/11$ |
| $\varphi_3$ | * | $3\pi/8$ | $\pi/4$ | $3\pi/16$ | $3\pi/20$ |
| $\varphi_4$ | * | $2\pi/5$ | $2\pi/7$ | $2\pi/9$ | $2\pi/11$ |
| $\varphi_5$ | * | * | $5\pi/12$ | $5\pi/16$ | $\pi/4$ |
| $\varphi_6$ | * | * | $3\pi/7$ | $\pi/3$ | $3\pi/11$ |
| $\varphi_7$ | * | * | * | $7\pi/16$ | $7\pi/20$ |
| $\varphi_8$ | * | * | * | $4\pi/9$ | $4\pi/11$ |
| $\varphi_9$ | * | * | * | * | $9\pi/20$ |
| $\varphi_{10}$ | * | * | * | * | $5\pi/11$ |

**RTHE theory.** The PWM signal depicted in Fig. 1,*c* exhibits both quarter-wave and half-wave symmetrical properties. To suppress $N$ harmonics and regulate the fundamental component, $(N+1)$ angles need to be calculated during each quarter period of the waveform.

To accomplish this objective, we will need to solve a system of transcendental equations using the Fourier series decomposition method:

$$I_1 = 1 + 2 \cdot \sum_{i=1}^{N+1} (-1)^i \cos(\varphi_i - \alpha_i) - M = 0; \qquad I_{N+1} = 1 + 2 \cdot \sum_{i=1}^{N+1} (-1)^i \cos((N+1)(\varphi_i - \alpha_i)) = 0, \tag{2}$$

for $k = 2(N+1) + 1$ and $M = \pi \cdot m_i / 4$, where $m_i$ is the modulation index (usually $0 \le m_i \le 1$). The term $\alpha_i$ is referred to as the perturbation angle and is denoted in radians. To ascertain the appropriate perturbation angles values $\alpha_i$ for any combination of $m_i$ and $k$, it is essential to

solve the set of transcendental equations as described in (2). This can be accomplished by employing various computational techniques, as introduced earlier.

In this study, we have employed the established GA algorithm. The fundamental procedures of GA are elaborated in [13]. A specific method for resolving the system of equations in (2) involves the minimization of the following constrained objective function:

$$F(\alpha_1,\alpha_2,\alpha_3,\ldots\alpha_{N+1}) = 0.5\left(I_1^2, I_2^2, I_3^2, \ldots, I_{N+1}^2\right), \quad (3)$$

where the constraint is defined by:

$$0 \le \varphi_1 - \alpha_1 \le \varphi_2 - \alpha_2 \le \varphi_3 - \alpha_3 \le \cdots \le \varphi_{N+1} - \alpha_{N+1} \le \pi/2\,. \quad (4)$$

The perturbation angles' numerical values for $m_i = 0.8$ can be found in Table 2, where $k = 9$ and 13.

Table 2

Numerical values of $\alpha_i$

| $\alpha_i$ | $k = 9$ | $k = 13$ |
|---|---|---|
| $\alpha_1$ | 0.1999 | 0.1341 |
| $\alpha_2$ | 0.2051 | 0.1477 |
| $\alpha_3$ | 0.4634 | 0.3071 |
| $\alpha_4$ | 0.3791 | 0.2899 |
| $\alpha_5$ | 0 | 0.4847 |
| $\alpha_6$ | 0 | 0.4153 |

To obtain the intended PWM signal, it is essential to establish a modified carrier signal using the perturbation angles computed through the minimization of (3). The carrier signal in question should have the capability to produce a PWM waveform that displays attributes of both odd and quarter-wave symmetries. It is expected to cross the horizontal axis (time axis) at the point $\pi$ and $2\pi$ [14].

The altered carrier signal takes on the subsequent expression:

$$f(\theta) = A_1 \cdot \sin(k_1 \cdot \theta) + A_2 \cdot \sin(k_2 \cdot \theta) + \cdots, \quad (5)$$

where $A_i$ and $k_i$ represent unidentified parameters.

The given formulation of $f(\theta_i)$ in this manuscript is characterized as follows:

$$f(\theta_i) = \sum_{i=1}^{N+1} C_i \cdot A_i, \quad C_i = \sin(q_i \cdot \theta), \quad (6)$$

where $C_i$ is the fixed value, $\theta_i = \varphi_i - \alpha_i$ and $q_i$ is the odd number within the range of [3, $k$].

Thus, the sole remaining unidentified parameters comprise $A_i$. This transforms the system into a set of linear equations that can be solved easily using standard techniques. Compared to [14, 15], the determination of the new points of intersection $\theta_i$ is performed exclusively over a quarter of a cycle.

As an illustration, let's take the case with $k = 9$. The set of algebraic equations for deriving the parameters $A_i$ can be expressed as:

$$\begin{aligned}
f(\theta_1) &= A_1 \sin(q_1\theta_1) + A_2 \sin(q_2\theta_1) + \\
&\quad + A_3 \sin(q_3\theta_1) + A_4 \sin(q_4\theta_1); \\
f(\theta_2) &= A_1 \sin(q_1\theta_2) + A_2 \sin(q_2\theta_2) + \\
&\quad + A_3 \sin(q_3\theta_2) + A_4 \sin(q_4\theta_2); \\
f(\theta_3) &= A_1 \sin(q_1\theta_3) + A_2 \sin(q_2\theta_3) + \\
&\quad + A_3 \sin(q_3\theta_3) + A_4 \sin(q_4\theta_3); \\
f(\theta_4) &= A_1 \sin(q_1\theta_4) + A_2 \sin(q_2\theta_4) + \\
&\quad + A_3 \sin(q_3\theta_4) + A_4 \sin(q_4\theta_4),
\end{aligned} \quad (7)$$

where

$$f(\theta_i) = \sin(\theta_i + \pi), \quad \theta_i = \varphi_i - \beta_i,$$

$i = 1, 2, 3, 4$ for $q_1 = 3$, $q_2 = 5$, $q_3 = 7$, $q_4 = 9$.

In general $k = n$: $q_1 = 3$, $q_2 = 5$, $q_3 = 7, \ldots$, $q_{(n-1)/2} = n$ (for quarter-wave symmetry).

The suggested approach can be succinctly outlined via a sequence of 5 steps, outlined as follows:

*1st step*: select the modulation index $m_i$ and define the quantity of harmonics $N$ to be regulated based on the $k$'s value;

*2nd step*: employ the GA algorithm to solve the non-linear algebraic transcendental equations (2) and ascertain the perturbation angles $\alpha_i$;

*3rd step*: utilize the calculated perturbation angles $\alpha_i$ to derive and solve the set of linear equations in $A_i$, employing (7);

*4th step*: create the intended modified carrier by inputting the numerical values of $A_i$ (calculated in 3rd step) and $q_i$ into (7); and

*5th step*: generate the PWM waveform.

**Results and discussion.** To evaluate the effectiveness of the suggested method, this section unveils the outcomes under the scenario where all harmonics until the 11th, 13th, and 17th orders are regulated in three phase inverters.

To derive the modulation signal ($\theta_i$, $f(\theta_i)$), which represents the modified carrier waveform, it is imperative to compute the $A_i$ values by solving a set of linear equations. Before this, the $\alpha_i$ perturbation angles are calculated by solving the nonlinear transcendental equations through the use of the GA. The resultant values are documented in Table 2.

The numeric values of the points of intersection $\theta_i$ and the associated modulation signal $f(\theta_i)$ for $m_i = 0.8$ and different values of $k$, specifically 9 and 13, can be found in Table 3. Substituting the values of ($\theta_i$, $f(\theta_i)$) into (7) results in a set of linear equations for $A_i$ corresponding to each $k$ value.

The solutions for $A_i$ with $k$ values of 9 and 13, are detailed in Table 4. Subsequently, by replacing the $q_i$ and $A_i$ values into (7), the modified carrier is derived, leading to the generation of the PWM waveform.

Table 3

Coordinates of intersection points

| $k = 9$ | | $k = 13$ | |
|---|---|---|---|
| $\theta_i$, rad | $f(\theta_i)$ | $\theta_i$, rad | $f(\theta_i)$ |
| 0.1782 | –0.1772 | 0.1276 | –0.1272 |
| 0.4434 | –0.4290 | 0.3010 | –0.2964 |
| 0.6995 | –0.6438 | 0.4782 | –0.4601 |
| 0.9008 | –0.7838 | 0.6076 | –0.5708 |
| * | * | 0.8242 | –0.7340 |
| * | * | 0.9310 | –0.8022 |

Table 4

Computed values of $A_i$

| | $k = 9$ | $k = 13$ |
|---|---|---|
| $A_1$ | –0.8027 | –0.8524 |
| $A_2$ | 0.5035 | 0.6133 |
| $A_3$ | –0.2283 | –0.3638 |
| $A_4$ | 0.0570 | 0.1694 |
| $A_5$ | 0 | –0.0559 |
| $A_6$ | 0 | 0.0099 |

The modified carrier, the output voltage waveform and its corresponding FFT are depicted in Figs. 2–4, respectively, for a frequency $f = 50$ Hz.

It is important to highlight that in a three phase voltage system, the corresponding phase shifts are 0, $-2\pi/3$ and $2\pi/3$, respectively. Consequently, for the alignment of our system voltages in phase:

- The reference sinusoid exhibit phase shifts of 0, $-2\pi/3$ and $2\pi/3$, respectively;
- the modified carrier exhibit phase shifts of $\pi$, $-q_i 2\pi/3+\pi$ and $q_i 2\pi/3+\pi$, respectively.

**Simulation results.** To showcase the effectiveness of a three phase inverter under various $k$ values (specifically, $k = 9$ and $k = 13$), custom carrier signals were generated. These custom carrier signals, along with their corresponding output voltage waveforms and resulting harmonic spectra, were simulated over a duration of 0.02 s. The simulations were carried out at a 50 Hz frequency and a DC input voltage of $V_{dc} = 100$ V.

As depicted by the simulation outcomes, the suggested approach has been effectively employed across various $k$ values. The outcomes of the simulation distinctly demonstrate that the modified carrier possesses half-and also quarter wave symmetry. As depicted in Fig. 2, the output voltages along with their corresponding harmonics spectra for the three phase inverter are illustrated in Fig. 3, 4, respectively. In conclusion the harmonic spectra provide clear evidence of the complete elimination of all fundamental frequency harmonics.

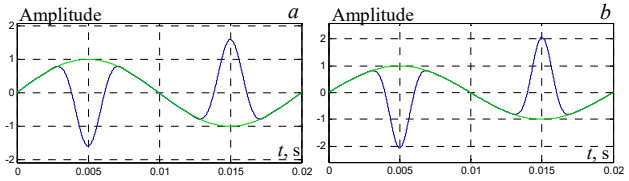


Fig. 2. The modified carrier, a sinusoidal reference in three phase inverter: $a$ – $k = 9$; $b$ – $k = 13$

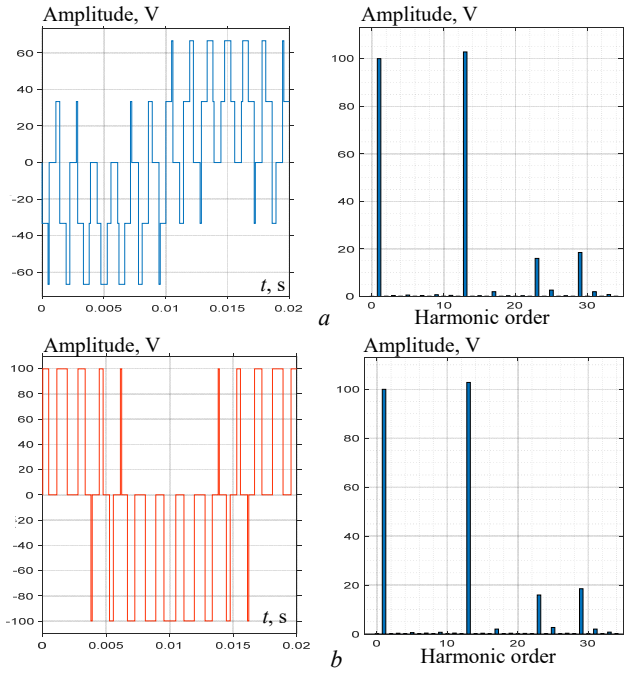


Fig. 3. Implementation of RTHE: $a$ – the phase-neutral output voltage waveform and FFT corresponding for $k = 9$; $b$ – line-to-line output voltage waveform and FFT corresponding for $k = 9$

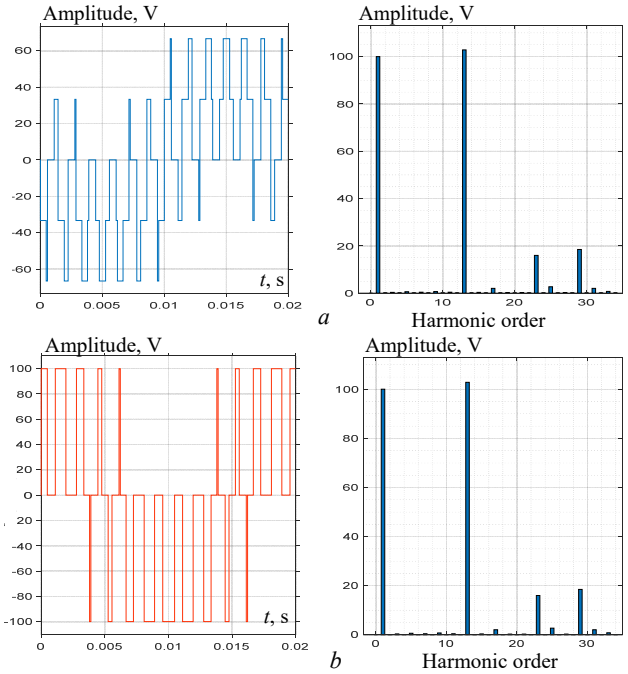


Fig. 4. Implementation of RTHE: $a$ – the phase-neutral output voltage waveform and FFT corresponding for $k = 13$; $b$ – line-to-line output voltage waveform and FFT corresponding for $k = 13$

**Experimental evaluation.** The practical execution of the experiment was realized using the Dspace DS1104. Figure 5 depicts the experimental prototype of the system; its purpose was to confirm the validity of the simulation results. The model comprises a DC power supply, Dspace 1104 for producing gating signals to control the switching devices and three phase inverter consists of 6 MOSFET IRF840 switches controlled by driver circuits

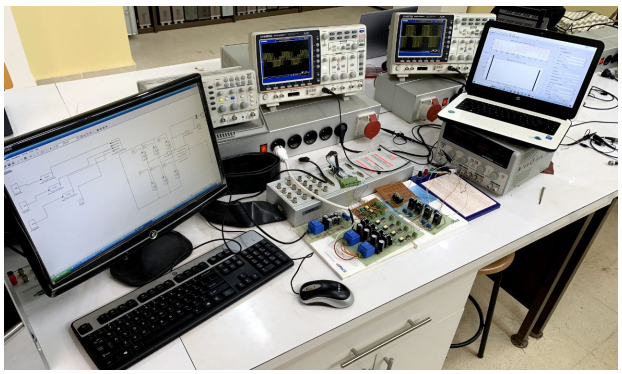

Fig. 5. Experimental prototype of the system

Figures 6,*a-c* show the experimental output voltage wave forms of the inverter, the phase-neutral voltage and the line-line voltage and their associated harmonic spectrum respectively. We note clearly that the harmonics 5th, 7th and 11th have been effectively eradicated.

Figures 7,*a-c* show the experimental output voltage wave forms of the inverter, the phase-neutral voltage and the line-line voltage and their associated harmonic spectrum respectively. We note clearly that the harmonics 5th, 7th, 11th, 13th and 17th have been effectively eradicated.

Figures 6, 7 illustrate congruence between the experimental results and simulations, providing compelling evidence to confirm the effectiveness of the proposed approach. The success in eliminating the specified harmonics clearly attests to the effectiveness of the suggested method.

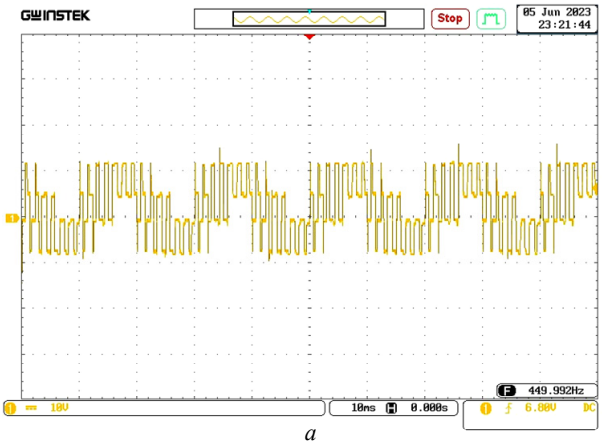


*a*

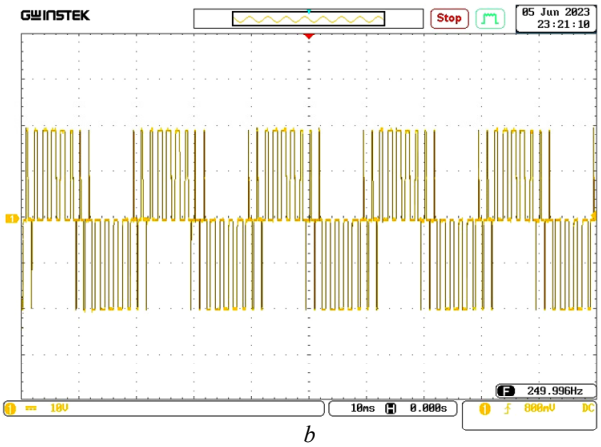


*b*

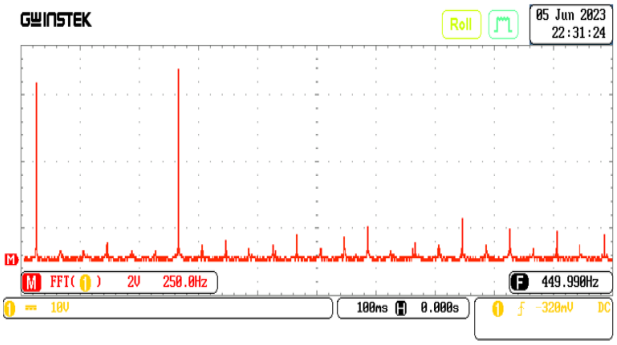


*c*

Fig. 6. Experimental implementation of RTHE:
*a* – the phase-neutral output voltage waveform for $k = 9$;
*b* – line-to-line output voltage waveform for $k = 9$;
*c* – harmonic spectrum

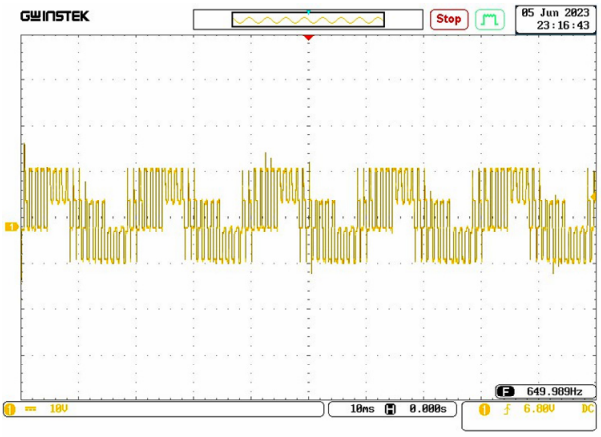


*a*

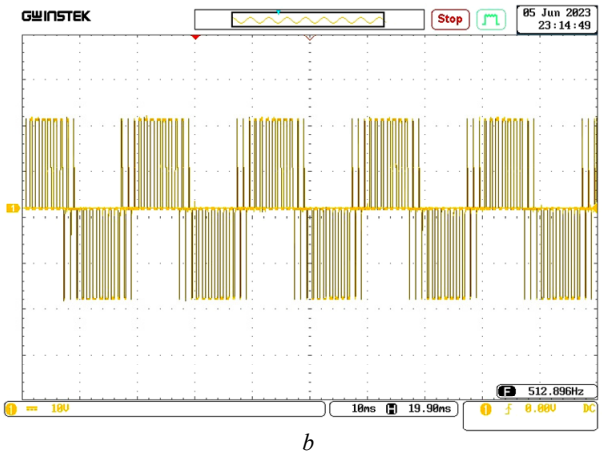


*b*

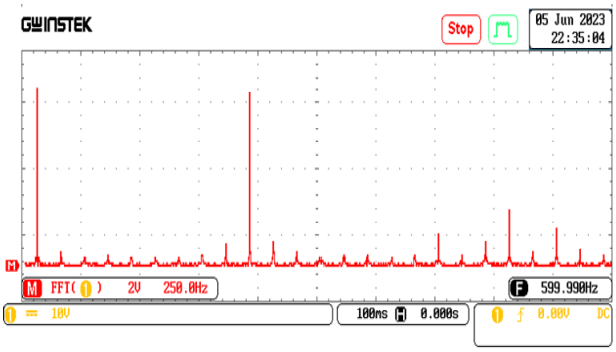


*c*

Fig. 7. Experimental implementation of RTHE:
*a* – the phase-neutral output voltage waveform for $k = 13$;
*b* – line-to-line output voltage waveform for $k = 13$;
*c* – harmonic spectrum

**Conclusions.**

1. This paper discusses a novel real-time implementation of SHE-PWM to eliminate the unwanted harmonics in the output voltage waveform of three phase inverter. This novel approach, known as RTHC, employs an alternative modulation strategy that streamlines the carrier generation process and facilitates the comparison between the carrier and the reference.

2. The suggested method commences by introducing a novel formula for the modified carrier waveform, resulting in a set of linear algebraic equations. To calculate the perturbation angles, the GA method is utilized. The perturbation angles have a crucial role in shaping the modified carrier. The proposed approach guarantees comprehensive control over both the elimination of harmonics and the fundamental component.

3. To evaluate the efficacy of the technique simulation and real-time hard ware implementations have been carried out. The simulation and experimental outcomes are highly satisfactory, conclusively demonstrating the soundness of the suggested approach. Presently, efforts are ongoing to develop solutions for the modified carrier waveform applicable across a broad spectrum in multi-level inverters.

**Conflict of interest.** The authors declare that they have no conflict of interest.

REFERENCES

***1.*** Toubal Maamar A.E. Analysis and Experimental Validation of Selective Harmonic Elimination in Single-Phase Five-Level Inverter using Particle Swarm Optimization Algorithm.

*Electronics*, 2022, vol. 26, no. 2, pp. 65-72. doi: https://doi.org/10.53314/ELS2226065M.
**2.** Toubal Maamar A.E., Helaimi M., Taleb R., Mouloudj H., Elamri O., Gadoum A. Mathematical Analysis of N-R Algorithm for Experimental Implementation of SHEPWM Control on Single-phase Inverter. *International Journal of Engineering Trends and Technology*, 2020, vol. 68, no. 2, pp. 9-16. doi: https://doi.org/10.14445/22315381/IJETT-V68I2P202.
**3.** Parimalasundar E., Kumar N.M.G., Geetha P., Suresh K. Performance investigation of modular multilevel inverter topologies for photovoltaic applications with minimal switches. *Electrical Engineering & Electromechanics*, 2022, no. 6, pp. 28-34. doi: https://doi.org/10.20998/2074-272X.2022.6.05.
**4.** Hosseinzadeh M.A., Sarbanzadeh M., Salgueiro Y., Rivera M., Wheeler P. Selective Harmonic Elimination In Cascaded H-Bridge Multilevel Inverter Using Genetic Algorithm Approach. *2019 IEEE International Conference on Industrial Technology (ICIT)*, 2019, pp. 1527-1532. doi: https://doi.org/10.1109/ICIT.2019.8755089.
**5.** Sakri D., Laib H., Farhi S.E., Golea N. Sliding mode approach for control and observation of a three phase AC-DC pulse-width modulation rectifier. *Electrical Engineering & Electromechanics*, 2023, no. 2, pp. 49-56. doi: https://doi.org/10.20998/2074-272X.2023.2.08.
**6.** Yaqoob M.T., Rahmat M.K., Maharum S.M.M., Su'ud M.M. A Review on harmonics elimination in real time for cascaded H-bridge multilevel inverter using particle swarm optimization. *International Journal of Power Electronics and Drive Systems (IJPEDS)*, 2021, vol. 12, no. 1, pp. 228-240. doi: https://doi.org/10.11591/ijpeds.v12.i1.pp228-240.
**7.** Mohammed L.A., Husain T.A., Ibraheem T.A.M. Implementation of SHE-PWM technique for single-phase inverter based on Arduino. *International Journal of Electrical and Computer Engineering (IJECE)*, 2021, vol. 11, no. 4, pp. 2907-2915. doi: https://doi.org/10.11591/ijece.v11i4.pp2907-2915.
**8.** Shanono I.H., Abdullah N.R.H., Daniyal H., Muhammad A. Optimizing performance of a reduced switch multi-level inverter with moth-flame algorithm and SHE-PWM. *The Journal of Engineering*, 2023, no. 11, pp. 1-27. doi: https://doi.org/10.1049/tje2.12281.
**9.** Hassan E.D., Mohammed K.G., Ali I.I. Implementation of TMS320f28335 DSP code based on SVPWM Technique for Driving VSI with Induction Motor. *International Journal of Power Electronics and Drive Systems (IJPEDS)*, 2022, vol. 13, no. 3, pp. 1895-1903. doi: https://doi.org/10.11591/ijpeds.v13.i3.pp1895-1903.
**10.** Yan X., Guan B., Du X. Multi-mode Hybrid Modulation Strategy for Three-level Converters based on Half-wave Symmetric SHEPWM. *2021 IEEE 12th Energy Conversion Congress & Exposition - Asia (ECCE-Asia)*, 2021, pp. 349-354. doi: https://doi.org/10.1109/ECCE-Asia49820.2021.9479391.
**11.** Bouyakoub I., Taleb R., Mellah H., Zerglaine A. Implementation of space vector modulation for two level Three-phase inverter using dSPACE DS1104. *Indonesian Journal of Electrical Engineering and Computer Science*, 2020, vol. 20, no. 2, pp. 744-751. doi: https://doi.org/10.11591/ijeecs.v20.i2.pp744-751.
**12.** Maamar A.E.T., Kermadi M., Helaimi M., Taleb R., Mekhilef S. An Improved Single-Phase Asymmetrical Multilevel Inverter Structure With Reduced Number of Switches and Higher Power Quality. *IEEE Transactions on Circuits and Systems II: Express Briefs*, 2021, vol. 68, no. 6, pp. 2092-2096. doi: https://doi.org/10.1109/TCSII.2020.3046186.
**13.** Ganesh Babu B., Surya Kalavathi M. Hardware Implementation of Multilevel Inverter using NR, GA, Bee Algorithms. *2021 International Conference on Sustainable Energy and Future Electric Transportation (SEFET)*, 2021, pp. 1-6. doi: https://doi.org/10.1109/SeFet48154.2021.9375750.
**14.** Guan B., Yan X. Hybrid low switching frequency modulation strategy with high dynamic response for high-power voltage source converter. *IET Electric Power Applications*, 2023, vol. 17, no. 7, pp. 906-917. doi: https://doi.org/10.1049/elp2.12312.
**15.** Chatterjee S., Das A. A review on technological aspects of different PWM techniques and its comparison based on different performance parameters. *International Journal of Circuit Theory and Applications*, 2023, vol. 51, no. 5, pp. 2446-2498. doi: https://doi.org/10.1002/cta.3513.

*Received 30.01.2024*
*Accepted 12.03.2024*
*Published 20.08.2024*

*L. Djafer*[1]*, PhD Student,*
*R. Taleb*[2]*, Professor,*
*F. Mehedi*[3]*, Associate Professor,*
[1] Electrical Engineering Department, Faculty of Technology, Hassiba Benbouali University of Chlef, Laboratoire Genie Electrique et Energies Renouvelables (LGEER), Chlef, Algeria,
e-mail: lem.djafer@gmail.com (Corresponding Author)
[2] Electrical Engineering Department, Faculty of Technology, Hassiba Benbouali University of Chlef, Laboratoire Genie Electrique et Energies Renouvelables (LGEER), and Unite de Recherche en Systemes Embarques de Chlef, Centre de Recherche sur l'Information Scientifique et Technique (CERIST), Chlef, Algeria,
e-mail: rac.taleb@gmail.com
[3] Faculty of Technology, Hassiba Benbouali University of Chlef, Laboratoire Genie Electrique et Energies Renouvelables (LGEER), Chlef, Algeria,
e-mail: f.mehedi@univ-chlef.dz

*How to cite this article:*
Djafer L., Taleb R., Mehedi F. Dspace implementation of real-time selective harmonics elimination technique using modified carrier on three phase inverter. *Electrical Engineering & Electromechanics*, 2024, no. 5, pp. 28-33. doi: https://doi.org/10.20998/2074-272X.2024.5.04